Effect of Cherenkov radiation on localized-state interaction

A. G. Vladimirov,[1,2,*] S. V. Gurevich,[3,4] and M. Tlidi[5]

[1]*Weierstrass Institute for Applied Analysis and Stochastics, Mohrenstrasse 39, D-10117 Berlin, Germany*

[2]*Lobachevsky State University of Nizhni Novgorod, pr. Gagarina 23, Nizhni Novgorod, 603950, Russia*

[3]*Institute for Theoretical Physics, University of Münster, Wilhelm-Klemm-Strasse 9, D-48149 Münster, Germany*

[4]*Center for Nonlinear Science (CeNoS), University of Münster, Corrensstrasse 2, 48149 Münster, Germany*

[5]*Faculté des Sciences, Université Libre de Bruxelles (U.L.B.), CP 231, Campus Plaine, B-1050 Bruxelles, Belgium*

(Received 13 July 2017; published 16 January 2018)

We study theoretically the interaction of temporal localized states in all fiber cavities and microresonator-based optical frequency comb generators. We show that Cherenkov radiation emitted in the presence of third-order dispersion breaks the symmetry of the localized structures interaction and greatly enlarges their interaction range thus facilitating the experimental observation of the dissipative soliton bound states. Analytical derivation of the reduced equations governing slow time evolution of the positions of two interacting localized states in a generalized Lugiato-Lefever model with the third-order dispersion term is performed. Numerical solutions of the model equation are in close agreement with analytical predictions.

DOI: 10.1103/PhysRevA.97.013816

I. INTRODUCTION

Frequency comb generation in microresonators has revolutionized such research disciplines as metrology and spectroscopy [1,2]. This is due to the development of laser-based precision spectroscopy, including the optical frequency comb technique [3]. Driven optical microcavities widely used for the generation of optical frequency combs can be modeled by Lugiato-Lefever equation [4] that possesses solutions in the form of localized structures also called cavity solitons (CSs) [5,6]. Localized structures of the Lugiato-Lefever model have been theoretically predicted in Ref. [7] and experimentally observed in Ref. [8]. In particular, temporal CSs manifest themselves in the form of short optical pulses propagating in the cavity. The experimental evidence of temporal CSs interaction performed in Ref. [8] indicated that due to a very fast decay of their tails, stable CS bound states are hardly observable. It has been also demonstrated theoretically and experimentally that when periodic perturbations [9–13] or high-order dispersions [13–17] are present, radiation of weakly decaying dispersive waves, e.g., so-called Cherenkov radiation [18–20], can lead to a strong increase of the interaction range and formation of new types of bound states. Experimental investigation of this radiation induced by the high-order dispersion was carried out in [10,13,14,16,21]. In particular, in Ref. [13] bound states of CSs resulting from their interaction via Cherenkov radiation were observed experimentally. Numerical studies of the effect of high-order dispersions on the properties of CSs and their interaction were reported in Refs. [10,13,14,17,19,22–26].

In this paper, we provide an analytical understanding of how two CSs interact under the action of the Cherenkov radiation induced by high order dispersion. For this purpose, we use the paradigmatic Lugiato-Lefever model with the third-order dispersion term. We derive the equations governing the time evolution of the position of two well-separated CSs interacting weakly via their exponentially decaying tails. We demonstrate that the presence of the third-order dispersion term breaking the parity symmetry of the model equation leads to a significant extension of the CS interaction range and affects strongly the nature of the interaction. We show that the interference between the dispersive waves emitted by two interacting CSs produces an oscillating pattern responsible for the stabilization of the bound states. In particular, we show that when two CSs interact, one of them remains almost unaffected by the interaction force. On the contrary, the second interacting CS is strongly altered by the dispersive wave emitted by the first one.

II. MODEL EQUATION

The generalized Lugiato-Lefever model with high-order dispersion terms has been introduced in Ref. [27]. In what follows, we consider only the second and third orders of dispersion. In this case, the intracavity field is governed by the following dimensionless equation:

$$\frac{\partial E}{\partial T} = E_{\rm in} - (1 + i\theta)E + id_2\frac{\partial^2 E}{\partial t^2} + d_3\frac{\partial^3 E}{\partial t^3} + iE|E|^2. \quad (1)$$

Here $E = E(t,T)$ is the complex electric field envelope, T is the slow time variable describing the number of round trips in the cavity, and t is the normalized retarded time variable (fast time). The parameter $E_{\rm in}$ denotes the normalized injected field amplitude, and θ is the normalized frequency detuning. Further, d_2 and d_3 are the second- and the third-order dispersion coefficients, respectively. Assuming anomalous group velocity dispersion $d_2 > 0$, we rescale d_2 to unity. Here we consider the case when $|d_3| \ll d_2 = 1$ and the fourth-order dispersion is much weaker than the third-order one. Therefore, we will neglect the effect of the fourth-order dispersion on the CS interaction.

*vladimir@wias-berlin.de

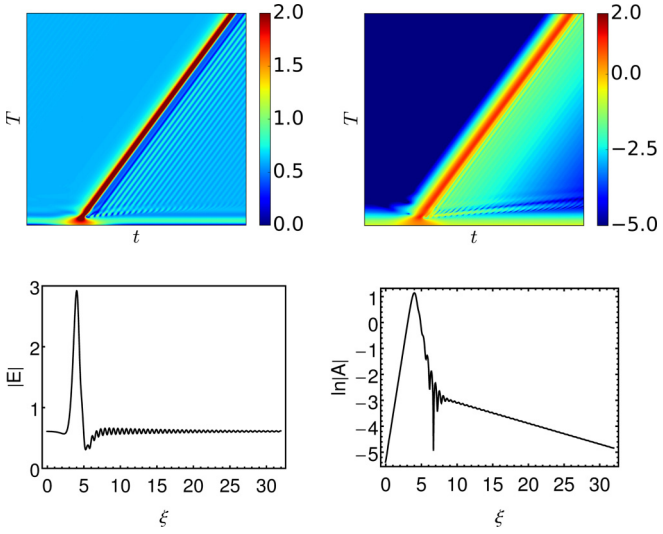

FIG. 1. The amplitude $|E|$ of a CS calculated by numerical solution of Eq. (1) in linear scale (left) and the deviation $A(\xi)$ of the CS amplitude from the background in logarithmic scale (right). Top: CS formation in the (t,T) plane ($d_3 = 0.2$). Bottom: CS moving uniformly with the velocity $v = 0.50679$ ($d_3 = 0.1$). Other parameters are $\theta = 3.5$ and $E_{\rm in} = 2.0$.

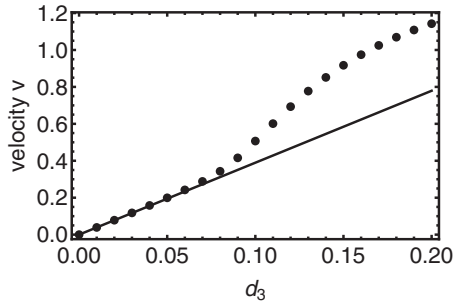

FIG. 2. Soliton velocity v vs. third-order dispersion coefficient d_3. Solid line corresponds to the plot of the asymptotic formula Eq. (2) with numerically calculated $s = 3.895$. Dots indicate soliton velocities obtained by means of direct numerical integration of Eq. (1) and by calculation of stationary soliton solutions in the comoving frame with the help of the Newtons iteration method. Parameter values are the same as in Fig. 1.

III. CAVITY SOLITON SOLUTION

The homogeneous stationary solution (HSS) of Eq. (1) is obtained from $E_{\rm in}^2 = I_0[1 + (\theta - I_0)^2]$ with $I_0 = |E_0|^2$. For $\theta < \sqrt{3}$ ($\theta > \sqrt{3}$) the HSS is monostable (bistable) as a function of the input intensity. When $d_3 = 0$, Eq. (1) supports both periodic [4] and CS [7] stationary states even in the monostable regime.

When $d_3 \neq 0$, due to the breaking of the parity symmetry $t \to -t$, CS becomes asymmetric and starts to move uniformly with the velocity v along the t axis. An example of a moving CS obtained by direct numerical simulations of Eq. (1) with periodic boundary conditions is shown in Fig. 1, where the deviation of the CS amplitude from the HSS is defined as $A(\xi) = E(\xi) - E_0$ with $\xi = t - vT$ (if not otherwise stated, all the data represented in the figures are dimensionless). It is seen from this figure that the inclusion of the third-order dispersion induces an asymmetry in CS shape. The left (leading) CS tail decays very fast to the HSS $E = E_0$ as in the case when the third-order dispersion is absent. By contrast, the right (trailing) tail contains a weakly decaying dispersive wave associated with the Cherenkov radiation [18]. Note that the phase matching condition between the CS and the linear dispersive wave leads to a resonant wave amplification [18,19], which is responsible for the appearance of this radiation. The relation between classical Cherenkov radiation and emission of dispersive waves by solitons is discussed in Ref. [18].

The velocity v of the CS can be estimated asymptotically at small d_3 using the multiple-scale techniques,

$$v \simeq -d_3 s, \quad s = \int_{-\infty}^{+\infty} \mathbf{w}_0 \cdot \frac{\partial^3 \mathbf{a}_0}{\partial \xi^3} d\xi \left(\int_{-\infty}^{+\infty} \mathbf{w}_0 \cdot \mathbf{a}_0 d\xi \right)^{-1}, \tag{2}$$

where the index "0" indicates that both the CS solution $\mathbf{a}_0 = (\mathrm{Re}A, \mathrm{Im}A)^T_{d_3=0}$ and the adjoint neutral mode $\mathbf{w}_0 = \mathbf{w}_{d_3=0}$ are evaluated at $d_3 = 0$. The soliton velocity estimated using Eq. (2) and calculated by numerical solution of the model Eq. (1) is shown in Fig. 2. It is seen that the asymptotic expression Eq. (2) with the numerically calculated coefficient $s = 3.895$ agrees very well with the results of direct numerical simulation of Eq. (1) for $d_3 \leqslant 0.1$, where the CS velocity depends linearly on the third-order dispersion coefficient. Notice that in the conservative limit where losses and injection are absent, one can obtain $s = \theta = 3.5$ [18]. At larger third-order dispersion coefficients, $d_3 \gtrsim 0.1$, analytical formula Eq. (2) underestimates the velocity v.

IV. CAVITY SOLITON TAILS

The CS shown in Fig. 1 is generated in regime where the system exhibits a bistable behavior. Let $E = E_0$ be the stable HSS with smallest field intensity $I_0 = |E_0|^2$. At large distance from the CS core its tails decay exponentially to this HSS. To characterize the asymptotic behavior of the CS tails, we substitute $E_0 + \epsilon b e^{\lambda\xi}$ into Eq. (1) and collect first-order terms in the small parameter ϵ. This yields the following characteristic equation:

$$d_3^2\lambda^6 + (1 + d_3 v)\lambda^4 - 2d_3\lambda^3 + \lambda^2(4I_0 + v^2 - 2\theta) - 2v\lambda + \theta^2 + 1 + 3I_0^2 - 4\theta I_0 = 0,$$

for the eigenvalue λ. In the absence of third-order dispersion, when $d_3 = 0$ and $v = 0$, four solutions of the characteristic equation are given by the expression $\lambda = \pm\sqrt{\theta - 2I_0 \pm \sqrt{I_0^2 - 1}}$. In the case when $I_0 < 1$ this expression gives two pairs of complex conjugated eigenvalues $\pm\lambda_0$ and $\pm\lambda_0^*$. For small nonzero d_3 the eigenvalues $\pm\lambda_0$ and $\pm\lambda_0^*$ are transformed into a pair of stable complex conjugated $\lambda_{1,2}$ and a pair of unstable complex conjugated (or real) eigenvalues, λ_5 and λ_6, located in small neighborhoods of $\pm\lambda_0$ and $\pm\lambda_0^*$ in the complex plane. More importantly, a pair of new eigenvalues, λ_3 and $\lambda_4 = \lambda_3^*$, appears. In the limit of small third-order dispersion $|d_3| \ll 1$ the eigenvalues $\lambda_{3,4}$ can

be written as

$$\lambda_{3,4} = -d_3 \mp i\left[\frac{1}{d_3} + d_3(\theta - 2I_0 - s)\right] + O\left(d_3^2\right),$$

where we have neglected the term $v^2 = O(d_3^2)$. These new eigenvalues with small real and large imaginary parts are associated with the weakly decaying linear dispersive wave (Cherenkov radiation) emitted by CSs. As we will see below, they are responsible for the increase of the CS interaction range and formation of a large number of bound states with large CS separations. In the anomalous dispersion regime, the dispersion coefficient d_3 is positive and the eigenvalues $\lambda_{3,4}$ have negative real parts. In this case the Cherenkov radiation appears at the trailing tail of the CS. At sufficiently large distances from the CS core this tail can be represented in asymptotic form,

$$A(\xi) \approx b_1 e^{\lambda_1 \xi} + b_2 e^{\lambda_2 \xi} + b_3 e^{\lambda_3 \xi} + b_4 e^{\lambda_4 \xi}, \quad \xi \to +\infty, \quad (3)$$

where the coefficients $b_{3,4}$ can be considered as amplitudes of the Cherenkov radiation. Furthermore, linearizing Eq. (1) at $E = E_0$ we obtain $b_{1,4} = p_{1,4} b_{2,3}^*$ with

$$p_{1,4} = \frac{E_0^2}{\theta - 2|E_0|^2 - i\kappa + iv\lambda_{1,4} - \lambda_{1,4}^2 + id_3\lambda_{1,4}^3}. \quad (4)$$

In particular, for the parameter values given in Fig. 1 and $d_3 = 0.1$ numerical estimation of $b_{2,3}$ and $p_{1,4}$ gives $b_2 = 3.286 + 1.581i$, $b_3 = -0.0678 + 0.0286i$, $p_1 = 0.0221 - 0.0856i$, and $p_4 = -0.001297 - 0.000895i$.

It follows from Eq. (4) that $|p_4| = O(d_3^2)$ in the limit $d_3 \to 0$, which means that small last term in Eq. (3) can be omitted in the asymptotic analysis of the CS interaction. Therefore, since the eigenvalue λ_3 has a small real part, at large positive ξ the third term in Eq. (3) with the amplitude b_3 dominates in the weakly decaying and oscillating CS trailing tail. This coefficient is exponentially small in the limit $d_3 \to 0$ and can be estimated analytically using the techniques similar to that described in the conservative limit [18,28]. This is, however, beyond the scope of the present work. Stable eigenvalues $\lambda_{5,6}$ are responsible for the fast decay of the CS leading edge at negative $\xi \to -\infty$:

$$A(\xi) \approx b_5 e^{\lambda_5 \xi} + b_6 e^{\lambda_6 \xi}, \quad \xi \to -\infty. \quad (5)$$

Numerical estimation gives the following values of the coefficients $b_{5,6}$: $b_5 = 0.111 - 1.50i$ and $b_6 = 3.54 + 4.83i$. Due to the translational invariance of Eq. (1) along the t direction, the linear operator $\hat{L}(\mathbf{a})$ with $\mathbf{a} = (\mathrm{Re}A\ ,\mathrm{Im}A)^T$ obtained by linearization of Eq. (1) on the CS solution has zero eigenvalue corresponding to the so-called neutral translational eigenmode $\mathbf{u} = \partial_\xi(\mathrm{Re}A\ ,\mathrm{Im}A)^T$ satisfying the relation $\hat{L}(\mathbf{a})\mathbf{u} = 0$. In what follows, we will need also the neutral mode $\mathbf{w}$ of the linear operator $\hat{L}^\dagger(\mathbf{a})$ adjoint to $\hat{L}(\mathbf{a})$, which satisfies the relation $\hat{L}^\dagger(\mathbf{a})\mathbf{w} = 0$. The asymptotic behavior of the function z defining the two components of the adjoint neutral mode $\mathbf{w} = (\mathrm{Re}z\ ,\mathrm{Im}z)^T$ is given by the relations

$$z(\xi) \approx c_1 e^{-\lambda_1^* \xi} + c_2 e^{-\lambda_2^* \xi} + c_3 e^{-\lambda_3^* \xi} + c_4 e^{-\lambda_4^* \xi}, \quad \xi \to -\infty, \quad (6)$$

$$z(\xi) \approx c_5 e^{-\lambda_5 \xi} + c_6 e^{-\lambda_6 \xi}, \quad \xi \to +\infty, \quad (7)$$

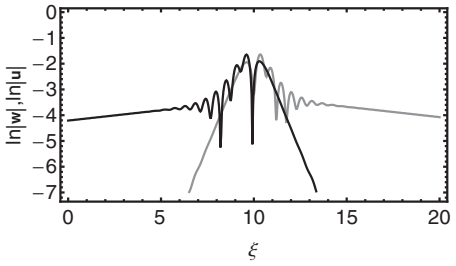

FIG. 3. Neutral mode $|\mathbf{u}|$ (gray) and adjoint neutral mode $|\mathbf{w}|$ (black) in logarithmic scale calculated for $d_3 = 0.1$. Other parameters are the same as for Fig. 1.

with $c_{1,4} = -p_{1,4}^* c_{2,3}^*$ and the coefficients $p_{1,4}$ defined by Eq. (4). Numerical estimation of the coefficients $c_{2,3,5,6}$ yields $c_2 = -0.313 + 0.252i$, $c_3 = -0.0152 - 0.0294i$, $c_5 = -0.185 - 0.0991i$, and $c_6 = 0.245 + 0.456i$. Similar to $|b_4| \ll |b_3|$, the absolute value of the coefficient c_4 is much smaller than that of c_3. Hence, the term proportional to c_4 can be neglected in Eq. (6) when deriving the CS interaction equations. Absolute values of the neutral mode $|\mathbf{u}| = |\partial_\xi A|$ and the adjoint neutral mode $|\mathbf{w}|$ are shown in Fig. 3 in logarithmic scale. From this figure we see that the neutral (adjoint neutral) mode has weakly decaying trailing (leading) tail.

V. INTERACTION EQUATIONS

To derive the CS interaction equations we use the Karpman-Solov'ev-Gorshkov-Ostrovsky approach [29] and look for the solution of Eq. (1) in the form of two weakly interacting CSs, see also Refs. [30,31],

$$E(\xi, T) = E_0 + A_1 + A_2 + \delta A. \quad (8)$$

Here, $A_k = A[\xi - \tau_k(T)]$, $k = 1, 2$ are unperturbed CS solutions with slowly changing coordinates along the ξ-axis, $d\tau_{1,2}/dT = O(\epsilon)$. The last term in the right-hand side describes a small correction due to the interaction, $\delta A = O(\epsilon)$, where the parameter $\epsilon \ll 1$ measures the weakness of the interaction. Substituting Eq. (8) into the model Eq. (1), collecting the terms of the first order in ϵ, writing solvability conditions of the resulting first-order equation, and using asymptotic relations (3), (5), (6), and (7) we obtain two equations governing the slow time evolution of the CS positions $\tau_{1,2}$:

$$\frac{d\tau_2}{dT} = \sum_{n=2,3} \mathrm{Re}\left[b_n c_n^* \left(v + 3d_3\lambda_n^2 + 2i\lambda_n\right) e^{\lambda_n \tau}\right], \quad (9)$$

$$\frac{d\tau_1}{dT} = -\sum_{n=5,6} \mathrm{Re}\left[b_n c_n^* \left(v + 3d_3\lambda_n^2 + 2i\lambda_n\right) e^{-\lambda_n \tau}\right] + \mathrm{Re}\left[\left(b_5 c_6^* + b_6 c_5^*\right)\left(v + \lambda_{56}^2 + i\lambda_{56} - \lambda_5\lambda_6\right) e^{-\frac{\lambda_{56}\tau}{2}}\right]. \quad (10)$$

Here $\tau = \tau_2 - \tau_1$ is the time separation of two CSs and $\lambda_{56} = \lambda_5 + \lambda_6$. At small time separations the term with $n = 2$ in the right-hand side of Eq. (9) and all the terms in the right-hand side of Eq. (10) dominate in the interaction equations. In particular, for $d_3 = 0.1$ when the eigenvalues $\lambda_{5,6}$ are real the two terms in Eq. (10) are responsible for monotonous attraction of first CS

to the second one. At larger CS separations, however, where the fast decaying right-hand side of Eq. (10) and the term with $n = 2$ in Eq. (9) become very small, the $n = 3$ term in the right-hand side of Eq. (9) related to the Cherenkov radiation becomes dominating. This slowly decaying term oscillates fast with the CS time separation and it is responsible for bound state formation at large τ. Thus, at large CS separations Eqs. (9) and (10) can be rewritten in the form clearly indicating the asymmetry of the CS interaction:

$$\frac{d\tau}{dT} \approx \frac{d\tau_2}{dT} \approx \mathrm{Re}\left[b_3 c_3^* \left(3d_3\lambda_3^2 + 2i\lambda_3\right) e^{\lambda_3 \tau}\right], \quad \frac{d\tau_1}{dT} \approx 0. \tag{11}$$

These equations predict the existence of an infinite countable set of equidistant stable CS bound states separated by unstable ones. The CS separations in the stable bound states are defined by the relation

$$\tau_n = \frac{\pi(2n+1) - \phi}{-\mathrm{Im}\lambda_3}, \tag{12}$$

with integer positive $n \geqslant n_0$, where odd (even) n correspond to stable (unstable) bound states and n_0 enumerates the bound state with minimal distance between the two CSs.

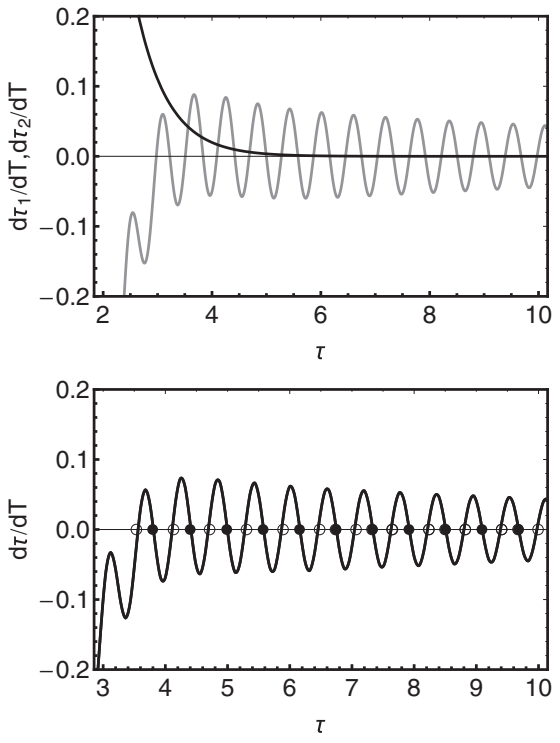

FIG. 4. Top: The dependence of CS velocities on their time separation. Unlike the velocity of the first CS (black line), which is positive and fast decaying with the increase separation $\tau = \tau_2 - \tau_1$, the velocity of the second CS (gray line) decays very slowly and oscillates fast as τ changes. Bottom: Difference of CS velocities as a function of their time separation. Zeros of this difference correspond to bound CS states. Numerically calculated CS time separations in the bound states are indicated by dots. Stable (unstable) bound states are shown by filled (empty) dots and correspond to decreasing (increasing) CS velocity difference. $d_3 = 0.1$, other parameters are the same as in Fig. 1.

The constant shift ϕ entering Eq. (11) is defined by $\phi = \arg\left[b_3 c_3^* (3d_3\lambda_3^2 + 2i\lambda_3)\right]$, where the product $b_3 c_3^*$ has to be calculated numerically. For $d_3 = 0.1$ and the parameter values of Fig. 1 the first bound state is unstable and corresponds to $n_0 = 12$ and numerical calculations give $b_3 c_3^* = (-0.162 + 2.433i) \times 10^{-3}$. The stable bound states calculated using Eq. (12) are in an excellent agreement with those calculated numerically with relative error less than 0.3%. Furthermore, for all bound states except for the first three stable bound states with smallest CS separations, τ_{13}, τ_{15}, τ_{17}, which are most strongly affected by short-range interaction associated with the fast-decaying eigenvalues λ_2, λ_5, and λ_6, the relative error is less than 0.1%. The smallness of the relative error indicates that the distances between the CS in the bound states are determined by the long range interaction via the Cherenkov radiation and are almost unaffected by the short-range interaction. The latter interaction is responsible only for the suppression of the bound state formation at small distances between the CS. In other words, the short-range interaction determined the number n_0 of the first bound state having the smallest CS separation. Note that Eq. (12) formally predicts the existence of infinite countable set of stable bound states. In reality the number of bound states is finite due to the finite cavity length and the presence of noise that can dominate over exponentially weak interaction at large CS separations.

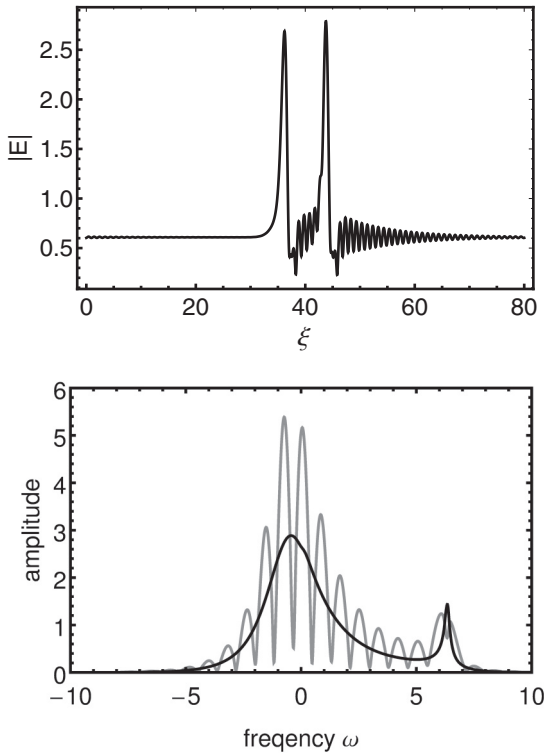

FIG. 5. Top: Stable bound state of two CSs calculated for $d_3 = 0.2$. Left CS is almost unaffected by the interaction while the right one has larger peak power and is much stronger modified by the interaction force. Note that for unstable bound states the peak power of the right CS is smaller than that of the left one. Bottom: Frequency comb envelope for a solitary pulse (black) and pulse bound state shown in left panel (gray). The envelope modulation period of the bound state comb is determined by the time separation of the two pulses. Other parameters are the same as in Fig. 1.

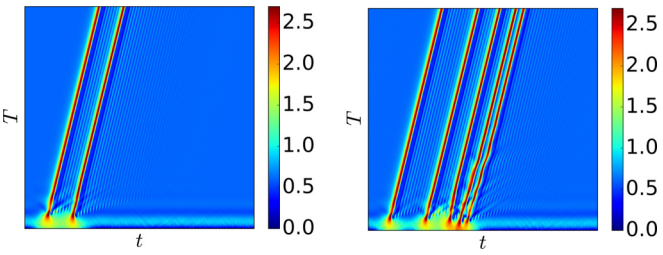

FIG. 6. Formation of bound states of two (left) and five (right) CSs calculated numerically for $d_3 = 0.2$. Other parameters are the same as in Fig. 1.

Long-range CS interaction Eqs. (11) indicate also that at large τ the first CS is almost unaffected by the interaction, while the second CS moves in the potential created by the first one. The velocities $d\tau_{1,2}/dt$ of the two interacting CSs calculated using Eqs. (9) and (10) with $d_3 = 0.1$ are shown in the top panel of Fig. 4 as functions of the CS time separation τ. The velocity of the first (left) CS defined by the right-hand side of Eq. (10) is a monotonous, always positive and fast decaying function of the CS time separation τ. By contrast, the velocity of the second (right) CS is negative only at relatively small τ and becomes slowly decaying and fast oscillating around zero at large τ. This fast oscillating behavior is related to the Cherenkov radiation and described by the $n = 3$ term in the right-hand side of Eq. (9). It is responsible for the formation of CS bond states at sufficiently large time separations τ. To find these states, we plot the difference of the CS velocities $d\tau/dt$ as a function of τ in the bottom panel of Fig. 4. Zeros of $d\tau/dt$ correspond to the fixed points of the CS interaction equations. Stable (unstable) CSs bound states calculated by direct numerical solution of the model Eq. (1) are indicated by filled (empty) dots in this figure. It is seen that they are in a good agreement with the results of the asymptotic analysis. Furthermore, a stable bound state of two CS and the corresponding frequency comb are shown in Fig. 5. The envelope modulation period of the bound state comb is determined by the time separation of the two pulses, see, e.g., Ref. [16]. Finally, a space-time diagram in the (T, t) plane illustrating the formation of two-soliton and five-soliton bound states with different distances is shown in Figs. 6(a) and 6(b).

IV. CONCLUSION

To conclude, we have investigated the effect of Cherenkov radiation on the CS interaction in the generalized Lugiato-Lefever model with the third-order dispersion term, which is widely used to describe frequency comb generation in optical microresonators and CS formation in fiber cavities. We have developed an analytical asymptotic theory of the CS interaction. The results of numerical simulation of the model equation are in good agreement with analytical predictions. We have shown that the third-order dispersion greatly enlarges the CS interaction range and makes the interaction very asymmetric. This allows for the stabilization of large number of bounded states formed by CSs. The appearance of the bound states is related to the long-range CS interaction mediated by the Cherenkov radiation, while the short-range CS interaction, which is only slightly modified by the Cherenkov radiation, is responsible for the suppression of bound-state formation at small distances between two CSs. As was mentioned above, in the absence of the third-order dispersion, bound states are hardly observable experimentally due to rather fast decay and slow oscillation of the CS tail [8]. That is, considering the system operating close to the zero dispersion wavelength regime where the third-order dispersion comes into play, one can facilitate experimental observation of the CS bound states. Finally, we note that the form of the CS interaction Eqs. (9), (10), and (11) depend on the symmetries of the model equation and asymptotic behavior of the CS tails, but not on the particular form of the nonlinear part of this equation. Therefore, the results of our analysis are applicable to a broad class of bistable optical systems with external driving beam. The results presented here could be also useful for qualitative understanding of the effect of the third and higher-order dispersion on the interaction of temporal CS in mode-locked lasers. However, due to the presence of an additional degree of freedom associated with the CS phase difference in the interaction equations, an in-depth theoretical analysis of this effect in active laser systems will be a subject of further research. Finally, the approach used here can be applied to study not only to the localized structures interaction, but also front interaction in bistable systems; see, e.g., Ref. [32].

ACKNOWLEDGMENTS

A.G.V. acknowledges the support of SFB 787, project B5 of the DFG, the Grant No. 14-41-00044 of the Russian Science Foundation, and Fédération Doeblin CNRS. S.V.G. acknowledges the support of Center for Nonlinear Science (CeNoS) of the University of Münster. M.T. thanks the Interuniversity Attraction Poles program of the Belgian Science Policy Office under Grant No. IAP P7-35. M.T. received support from the Fonds National de la Recherche Scientifique (Belgium).

[1] T. J. Kippenberg, R. Holzwarth, and S. A. Diddams, Science **332**, 555 (2011).
[2] F. Ferdous, H. Miao, D. E. Leaird, K. Srinivasan, J. Wang, L. Chen, L. T. Varghese, and A. M. Weiner, Nat. Photon. **5**, 770 (2011).
[3] T. W. Hansch, Rev. Mod. Phys. **78**, 1297 (2006).
[4] L. A. Lugiato and R. Lefever, Phys. Rev. Lett. **58**, 2209 (1987).
[5] S. Coen and M. Erkintalo, Opt. Lett. **38**, 1790 (2013).
[6] T. Herr, V. Brasch, J. D. Jost, C. Y. Wang, N. M. Kondratiev, M. L. Gorodetsky, and T. J. Kippenberg, Nat. Photon. **8**, 145 (2014).
[7] A. J. Scorggie, W. J. Firth, G. S. McDonald, M. Tlidi, R. Lefever, and L. A. Lugiato, Chaos, Solitons Fractals **4**, 1323 (1994).
[8] F. Leo, S. Coen, P. Kockaert, S.-P. Gorza, P. Emplit, and M. Haelterman, Nat. Photon. **4**, 471 (2010).

[9] J. M. Soto-Crespo, N. Akhmediev, P. Grelu, and F. Belhache, Opt. Lett. **28**, 1757 (2003).
[10] M. Olivier, V. Roy, and M. Piché, Opt. Lett. **31**, 580 (2006).
[11] D. Turaev, A. G. Vladimirov, and S. Zelik, Phys. Rev. Lett. **108**, 263906 (2012).
[12] E. Berrios-Caro, M. G. Clerc, and A. O. Leon, Phys. Rev. E **94**, 052217 (2016).
[13] Y. Wang, F. Leo, J. Fatome, M. Erkintalo, S. G. Murdoch, and S. Coen, Optica **4**, 855 (2017).
[14] F. Leo, A. Mussot, P. Kockaert, P. Emplit, M. Haelterman, and M. Taki, Phys. Rev. Lett. **110**, 104103 (2013).
[15] C. Milián, D. V. Skryabin, Opt. Express **22**, 3732 (2014).
[16] V. Brasch, M. Geiselmann, T. Herr, G. Lihachev, M. H. P. Pfeiffer, M. L. Gorodetsky, and T. J. Kippenberg, Science **351**, 357 (2016).
[17] P. Parra-Rivas, D. Gomila, P. Colet, and L. Gelens, Eur. Phys. J. D **71**, 198 (2017).
[18] N. Akhmediev and M. Karlsson, Phys. Rev. A **51**, 2602 (1995).
[19] D. V. Skryabin and A. V. Gorbach, Rev. Mod. Phys. **82**, 1287 (2010).
[20] A. V. Cherenkov, V. E. Lobanov, and M. L. Gorodetsky, Phys. Rev. A **95**, 033810 (2017).
[21] J. K. Jang, M. Erkintalo, S. G. Murdoch, and S. Coen, Opt. Lett. **39**, 5503 (2014).
[22] M. Tlidi and L. Gelens, Opt. Lett. **35**, 306 (2010).
[23] M. Tlidi, L. Bahloul, L. Cherbi, A. Hariz, and S. Coulibaly, Phys. Rev. A **88**, 035802 (2013).
[24] L. Bahloul, L. Cherbi, A. Hariz, and M. Tlidi, Phil. Trans. R. Soc. A **372**, 20140020 (2014).
[25] P. Parra-Rivas, D. Gomila, F. Leo, S. Coen, and L. Gelens, Opt. Lett. **39**, 2971 (2015).
[26] H. Taheri, A. B. Matsko, and L. Maleki, Eur. Phys. J. D **71**, 153 (2017).
[27] M. Tlidi, A. Mussot, E. Louvergneaux, G. Kozyreff, A. G. Vladimirov, and M. Taki, Opt. Lett. **32**, 662 (2007).
[28] V. I. Karpman, Phys. Rev. E **47**, 2073 (1993).
[29] K. A. Gorshkov and L. A. Ostrovsky, Physica D **3**, 428 (1981).
[30] A. G. Vladimirov, J. M. McSloy, D. V. Skryabin, and W. J. Firth, Phys. Rev. E **65**, 046606 (2002).
[31] M. Tlidi, A. G. Vladimirov, and P. Mandel, IEEE J. Quant. Electron. **39**, 216 (2003).
[32] M. G. Clerc and C. Falcon, Physica A **356**, 48 (2005).